Synthesis and Characterization of Li^+ ions substituted $MnFe_2O_4$ Nanoparticles

B.Padma[1,*], T. Balu[2], M. Daniel Sweetlin[3], G. Vasuki[2]

Received Date: 12/04/2023 ***Revised Date: 21/05/2023*** ***Accepted Date: 10/06/2023***

[1]Research Scholar, Reg. No: 19121272132001, Department of Physics, St. John's College, Palayamkottai, affiliated to Manonmaniam Sundaranar University, Abishekapatti, Tirunelveli – 627012, Tamilnadu, India.

[2]Aditanar college of Arts and Science, Tiruchendur, affiliated to Manonmaniam Sundaranar University,Abishekapatti, Tirunelveli – 627012, Tamilnadu, India.

[3]St. John's College, Palayamkottai, affiliated to Manonmaniam Sundaranar University,Abishekapatti, Tirunelveli – 627012, Tamilnadu, India.

Abstract

Lithium manganese nanoferrites ($Li_xMn_{1-2x}Fe_{2+x}O_4$, x = 0.0, 0.1, 0.2, 0.3, 0.4) are synthesized by chemical co-precipitation technique. Structure, morphology and nature of chemical bonding are analysed through Powder X-ray Diffraction (PXRD), Scanning Electron Microscope (SEM) and Fourier Transform Infrared Spectrograph (FTIR) respectively. From PXRD spectra the cubic spinel nanostructure of the synthesized samples are studied. From PXRD data, the crystallite size and various structural parameters such as lattice constant, volume of a cubic unit cell, X-ray density, hopping lengths of the samples are calculated and compared. Also specific surface area, dislocation density and microstrain of the samples are calculated. The surface morphology of the synthesized sample is studied through SEM images. The positions of octahedral and tetrahedral sites are identified from the vibrational bands in FTIR spectra.

Keywords: nanostructure, co-precipitation, PXRD, SEM

1. Introduction

Nanoferrites have attracted researchers for the past several years on account of their massive applications in various fields. Due to their remarkable qualities such as quantum size effect, large surface to volume ratio, chemical stability and superparamagnetism, they play a vital role in the field of bio-medicine and electronics. The various properties like mechanical properties, electrical properties, optical properties, thermal properties, magnetic properties of bulk materials are very much altered due to their reduction in size to nanometre scale [1-3].The general formula of ferrite is AFe_2O_4 where A is a divalent metal ion such as Ni, Co, Mn, Mg etc. Nanoferrites can be synthesized by various methods such as co-precipitation route [4], sol-gel method [5], hydrothermal route [6], glycine-assisted combustion technique [7].The properties of the nanoferrites are strongly dependent on the preparation

methods, the amount of doping and doping material. Many researchers have tried to enhance the property of nanoferrites by doping transition metal ions such as Cd^{2+}, Cr^{2+}, Cu^{2+}, Mn^{2+}, Ni^{2+}, Zn^{2+}.Talaat M. Hammad et al studied the impact of Mg^{2+} doping on optical, structural and magnetic properties of copper nanoferrites and it has been found that as the Mg^{2+} concentration increases, the band gap energy of copper nanoferrites increases and the saturation and remanent magnetization decreases [8]. Thomas Dippong et al studied the effect of transition metal doping on the structural, morphological and magnetic properties of $NiFe_2O_4$. They have found that the particles size of $NiFe_2O_4$ increases by doping with Mn^{2+} and decreases by doping with Zn^{2+} and Co^{2+} ions respectively [9].Ch. Komali et al studied the effect of Cu^{2+} substitution on structure, morphology and magnetic properties of Mg-Zn spinel ferrite. Their results show that the saturation magnetization increases and coercivity decreases with increase in Cu^{2+} concentration in Mg-Zn nanoferrites [10]. Pawar A.D et al studied the effect of Ag doping on DC electrical resistivity and antimicrobial activity of copper-zinc nanoferrites and it is shown that the inhibitory zone of Cu-Zn nanoferrites increases with increasing silver doping [11]. Manganese nanoferrites have attracted many researchers due to their mixed spinel structure, soft magnetic nature and mechanical stability. Due to its good biocompatibility and superparamagnetic nature, manganese nanoferrites play a vital role in the biomedical applications like targeted drug delivery [12]. Lithium nanoferrites can be used for the formation of super capacitors and lithium ion batteries [13].

A few detailed research work has been observed on mixed lithium manganese nanoferrites. Hence this present study aims to synthesize $Li_xMn_{1-2x}Fe_{2+x}O_4$ (x = 0.0, 0.1, 0.2, 0.3, 0.4) by co-precipitation technique and to investigate the structural and morphological properties.

2. Materials and methods

All the reactant salts used in the synthesis process are of AR grade. Lithium manganese nanoferrites ($Li_xMn_{1-2x}Fe_{2+x}O_4$, x = 0.0, 0.1, 0.2, 0.3, 0.4) are synthesized by chemical co-precipitation technique. Li^+, Mn^{2+} and Fe^{3+}sulphate salt solutions are taken in the required ratio and stirred continuously using a magnetic stirrer for 30 minutes to obtain the starting solution (pH~3). 3M solution of sodium hydroxide (NaOH) is prepared as precipitant and is slowly added in drops to the starting

solution until the pH level reaches 10.5. The resulting dark green precipitate is stirred continuously for 2 hours maintaining a temperature of 70°C to obtain a uniform phase of nanomaterial. The obtained dark brown precipitate is then cooled to room temperature and washed repeatedly with deionized water, filtered and dried at 105°C. Then it is grinded well to get lithium manganese nanoferrite powder. Figure 1 below shows a schematic flow diagram of the synthesis process.

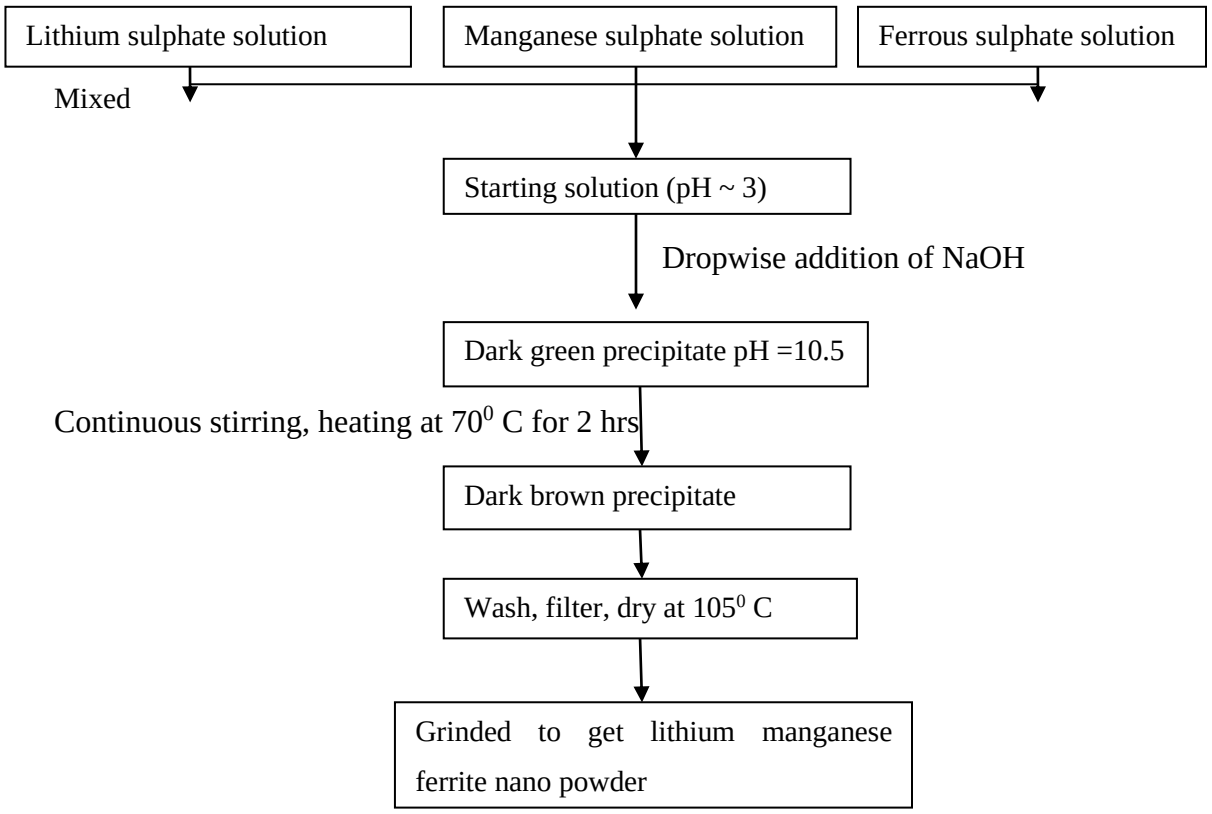

Figure 1: Flow diagram for synthesizing lithium manganese nanoferrites

All the asprepared samples are then subjected to various characterization studies to investigate their properties. The structural and morphological studies are carried out using Powder X-ray Diffraction Technique (PXRD), Scanning Electron Microscopy (SEM) and Fourier Transform Infrared Spectroscopy (FTIR).

3. Results and Discussions

3.1 Powder X – ray diffraction

Powder X-ray diffraction is an analytical technique used for phase identification of a crystalline material and can provide information on unit cell dimensions [14]. The X-ray diffraction pattern of the samples is shown in figure 2. All the as-synthesized samples show prominent peaks at 2θ which agrees with JCPDS 74-2403 of $MnFe_2O_4$ [15] and JCPDS 82-1436 of $LiFe_2O_4$ [16]. This confirms the cubic spinel ferrite nanostructure of the as-synthesized nanomaterials. The calculated values of various structural parameters are given in table 1.

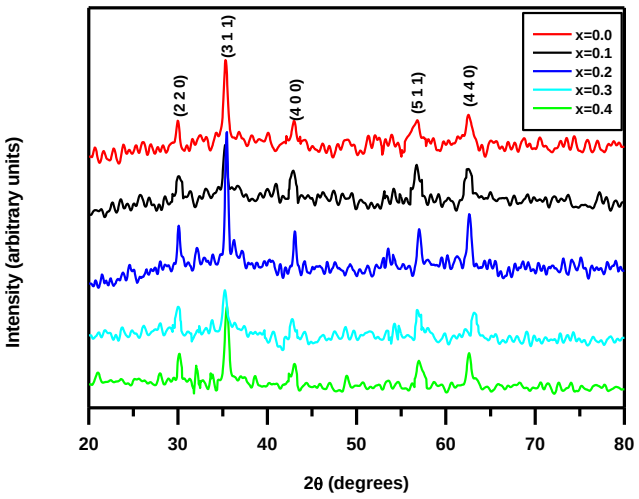

Figure 2 PXRD pattern of $Li_xMn_{1-2x}Fe_{2+x}O_4$ (x = 0.0, 0.1, 0.2, 0.3, 0.4)

From PXRD data,

the lattice constant 'a'is calculated using the relation

$$a = d\,(h^2+k^2+l^2)^{1/2} \quad (1)$$

where

d is the lattice spacing

h, k, l are the miller indices corresponding to the prominent peak.

The volume of a unit cell is given by

$$V=a^3 \quad (2)$$

The X-ray density (ρ_x) is calculated using the expression

$$\rho_x = 8M / Na^3 \quad (3)$$

where M is the molecular weight of the sample and N is the Avogadro's number whose value is 6.023 x 10^{23} mol^{-1}. The samples are pelletized and their bulk density (ρ_b) is calculated using the relation

$$\rho_b = m/\pi r^2 h \quad (4)$$

where m is the mass, r is the radius and h is the thickness of the pellet. It is found that the bulk density is smaller than the X-ray density which indicates the presence of pores in all the synthesized ferrite samples.

The percentage of porosity (p) is calculated using the relation

$$p = (1 - \rho_b/\rho_x) \times 100 \quad (5)$$

The high values of porosity percentage show that these ferrite samples can be used as gas sensors [17].

The distance between magnetic ions or hopping length of tetrahedral site (L_A) and octahedral site (L_B) are calculated from lattice constant a using the relations:

$$L_A = \sqrt{3}\, a / 4 \quad (6)$$

$$L_B = \sqrt{2}\, a / 4 \quad (7)$$

The average crystallite size is calculated using Debye Scherrer formula

$$D = 0.9\lambda / \beta \cos\theta \quad (8)$$

where λ is the wavelength of Cuk_α radiation, β is the full width at half maximum intensity of the peak, θ is the Bragg's angle.

Specific surface area(S) which is defined as the total surface area of a material per unit mass is calculated for the cubic ferrite samples using the following relation

$$S = 6000/\rho_x D \quad (9)$$

The number of dislocations in a unit volume of crystalline material which is called the dislocation density (ρ_D) is calculated using the relation

$$\rho_D = 1/D^2 \quad (10)$$

The microstrain (ε_s) which is defined as the root mean square variations of the lattice parameter across the crystallite due to presence of defects and stress, is calculated using the relation

$$\varepsilon_s = \beta/4\tan\theta \quad (11)$$

Table 1: Structural parameters calculated using XRD data

Structural parameter	Sample				
	$Mn_{1.0}Fe_{2.0}O_4$	$Li_{0.1}Mn_{0.8}Fe_{2.1}O_4$	$Li_{0.2}Mn_{0.6}Fe_{2.2}O_4$	$Li_{0.3}Mn_{0.4}Fe_{2.3}O_4$	$Li_{0.4}Mn_{0.2}Fe_{2.4}O_4$
d(Å)	2.5465	2.5429	2.5428	2.5330	2.5307
a(Å)	8.446	8.434	8.433	8.401	8.394
V(Å)^3	602.47	599.94	599.71	592.93	591.33
ρ_x(g/cm)^3	5.08	4.99	4.78	4.63	4.43
ρ_b(g/cm)^3	3.82	3.75	3.63	3.57	3.54
p (%)	24.8	23.5	20.1	17.5	13.8
L_A (Å)	3.653	3.652	3.651	3.637	3.634
L_B (Å)	2.986	2.982	2.981	2.970	2.968
D (nm)	28.25	28.25	28.26	28.27	42.41
S x 10^3 (m^2/g)	41.8	42.56	44.17	45.84	31.94
ρ_D x 10 ^{14} (m^{-2})	12.53	12.53	12.52	12.51	5.56
ε x 10^{-3}	4.05	4.04	4.05	4.03	2.68

As hopping length purely depends on the lattice constant, the value of hopping length of tetrahedral site is always greater than the value of octahedral site due to the difference in the distance between Fe^{3+} and O^{2-} ions of two sites. The lattice constant decreases with Li^+ substitution due to replacement of larger cation, Mn^{2+}. It is to be noted here that the ionic radii of Fe^{3+}, Li^+ and Mn^{2+} are

0.49 Å, 0.59Å and 0.66Å respectively, in the tetrahedral site and 0.64Å, 0.76Å and 0.83Å respectively in the octahedral site [18].

The average crystallite size of the samples is in the range from 28.25 nm to 42.41nm.It is observed that the particle size shows a large variation as the concentration of Li^+ ion becomes greater than 0.3 i.e. at x = 0.4. This shows that the effect of doping Li^+ ions to manganese ferrites are favourable only upto x = 0.3.

Due to nanosize of the particles, the surface area per unit mass is found to have larger values. The large values of the specific surface area show that all the synthesized ferrite samples have better reactivity with the surrounding particles compared to their bulk counterpart [19]. The high value of the dislocation density of the samples shows the large strength of the materials. The microstrain values of the samples are also found to be high due to the nanosized particles present in the samples.Also these values are found to decrease with the increase in the concentration of Li^+ ions. A very large decrease in specific surface area and microstrain has been observed for Li^+ concentration at x=0.4 due to large particle size.

3.2 Scanning Electron Microscopic analysis

The morphology of the synthesized samplesis studied by using scanning electron microscope.The SEM images of the synthesized samples for various resolutions (1μm, 2μm and 5μm) are taken. The SEM images of the samples for 1μm resolution are shown in figures 3(a-e).

The SEM images show spherical morphology of the samples. Agglomerations are observed which are due to strong magnetic interaction between the synthesized ferrite nanoparticles [20].

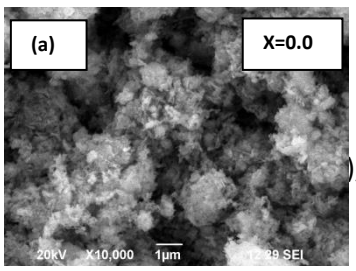

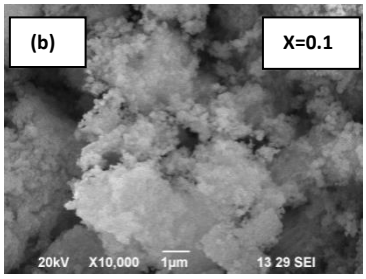

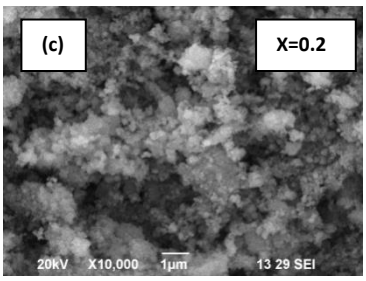

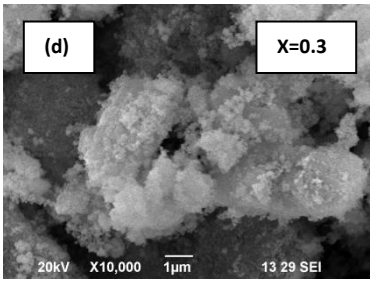

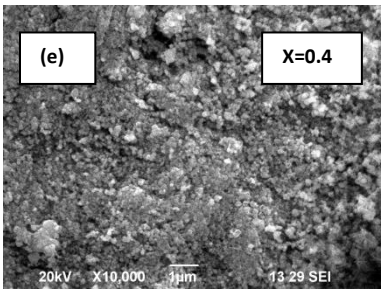

Figures 3(a - e) SEM images of $Li_xMn_{1-2x}Fe_{2+x}O_4$nanoparticles

3.3 Fourier Transform Infrared analysis

Fourier Transform Infrared (FTIR) spectroscopy is an important characteristic technique which provides information regarding the structure of a material. Figure 4 compares the FTIR spectra of the as-synthesized samples observed in the range of 4000 – 400 cm^{-1}.

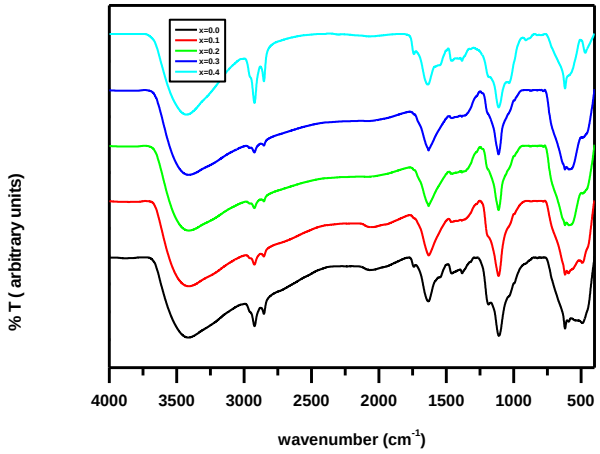

Figure 4 FTIR spectra of $Li_xMn_{1-2x}Fe_{2+x}O_4$ (x = 0.0, 0.1, 0.2, 0.3, 0.4)nanoparticles

The spectra show different peaks which are attributed to different functional groups. Two major absorption bands are found around 600 $cm^{-1}$and 450 cm^{-1} in all the five samples. The higher frequency band found at 625 cm^{-1}, 610 cm^{-1}, 602 cm^{-1}, 593 cm^{-1} and 616 $cm^{-1}$for $Li_xMn_{1-2x}Fe_{2+x}O_4$ (x = 0.0, 0.1, 0.2, 0.3, 0.4) respectively is due to the intrinsic vibration of metal – oxygen bond in the tetrahedral site and thelower frequency band found at 484 cm^{-1}, 484 cm^{-1}, 452 cm^{-1}, 452 cm^{-1} and 461 cm^{-1} for $Li_xMn_{1-2x}Fe_{2+x}O_4$ (x = 0.0, 0.1, 0.2, 0.3, 0.4) respectively is caused by metal – oxygen vibration in octahedral site. Hence, the FTIR results confirm the single phase spinel structure formation having two sub lattices; octahedral site and tetrahedral site of the prepared samples [21].

The bands appearing around 3400 cm^{-1} represents the O – H stretching vibration and1100 cm^{-1} represents the O – H bending vibration, which indicates the presence of free or absorbed water moleculesand it reveals the presence of hydroxyl groups in the as-synthesized samples [22].

4. Conclusions

Lithium manganese nanoferrites$Li_xMn_{1-2x}Fe_{2+x}O_4$ (x = 0.0, 0.1, 0.2, 0.3, 0.4) are synthesized by chemical co-precipitation technique. The cubic spinel nanoferrite structure of the as-synthesized samples is confirmed by powder X-ray diffraction analysis. The average particle size is in nanometres.

The spherical morphology of the samples is viewed from the SEM images.The FTIR spectra show the presence of tetrahedral and octahedral sites in all the synthesized samples and hence confirm the cubic spinel nanostructure of the samples.

Acknowledgements

The authors are thankful to Alagappa University, Karaikudi, Archbishop Casimir Instrumentation center, Trichy, SAIF, Karunya Institute of Technology and Sciences, Coimbatore for providing excellent instrumentation facilities.

References

1. Filho A.G.S & Fagan S.B, 'Nanomaterials Properties In: Bergmann, C.P., de Andrade, M.J. (eds) Nanostructured Materials for Engineering Applications', Springer, Berlin,5-22 (2011).
2. Arivalagan K, Ravichandran S, Rangasamy K, & Karthikeyan E, 'Nanomaterials and its Potential Applications', International Journal of ChemTech Research, 3, 534-538 (2011).
3. Gajanan K, Tijare S.N, 'Applications of Nanomaterials', Materials Today Proceedings,5, 1093-1096 (2018).
4. N.D Kandpal, N. Sah, R. Loshali & J. Prasad, 'Co-precipitation Method of Synthesis and Characterisation of Iron Oxide Nanoparticles', Journal of Scientific and Industrial Research, 73, 87-90 (2014).
5. Lavanya Khanna & Tripathi S.K, 'Effect of Temperature on the Structural, Morphological and Magnetic Properties of Magnesium Ferrite Nanoparticles',Research Journal of Recent Sciences,6, 1-9 (2017).
6. Chien-Yie Tsay, Yi-ChunCchiu & Chien-MingLei, 'Hydrothermally synthesizedMg-Based Spinel Nanoferrites: Phase Formation and Study on Magnetic Features and Microwave Characteristics', Materials,11, 2274-2284 (2018).
7. Deraz N.M, 'Construction of $Mn_{0.5}Mg_{0.5}Fe_2O_4$ Nanoparticles', Egypt. J. Chem.,61, 531-538 (2018).
8. Talaat M. Hammad, S. Kuhn, Ayman Abu Amsha, Nasser K. Hejazy, R. Hempelmann, " Comprehensive Study of the Impact of Mg^{2+} Doping on Optical, Structural and Magnetic

Properties of Copper Nanoferrites, Journal of Superconductivity and Novel Magnetism, 33, 3065-3075 (2020).

9. Thomas Dippong, Oana Cadar, Erika Andrea Levei, "Effect of Transition Metal Doping on the Structural, Morphological and Magnetic Properties of $NiFe_2O_4$", Materials, 15, 1-14 (2022).
10. Ch. Komali, N. Murali, D. Parajuli, A. Ramakrishna, Y. Ramakrishna, K. Chandramouli, "Effect of Cu^{2+} substitution on Structure, Morphology and Magnetic Properties of Mg-Zn Spinel Ferrite", Indian Journal of Science and Technology ,14, 2309-2316 (2021).
11. Pawar A.D, Patil B.B, Salunkhe A.K, Shinde T.J, Bhongale S.R, Kumar S, "Effect of Ag Doping on Dc Electrical Resistivity, Thermoelectric Power, VSM Analysis and Antimicrobial Activity of Copper-Zinc Nanoferrites', Indian Journal of Physics, 96, 3161-3176 (2021).
12. Thomas Dippong, Erika Andrea Levei, Oana Cadar, 'Recent Advances in Synthesis and Applications of MFe_2O_4 (M = Co, Cu, Mn, Ni, Zn) Nanoparticles', Nanomaterials, 11, 1-33 (2021).
13. Mukhtar Ahmad, Muhammad Shahid, yousef Mohammad Alanazi, Atiq ur Rehman, Muhammad Asif & Charles W. Duhnill, 'Lithium Ferrite ($Li_{0.5}Fe_{2.5}O_4$): Synthesis, Structural, Morphological and Magnetic Evaluation for Storage Devices', Journal of Materials Research and Technology, 8, 3386-3395 (2022).
14. Wei Zhang, Aimin Sun, Xiaoguang Pan, Yingqiang Han, Xiqian Zhao, Lichao Yu, Zhuo Zuo & Nanzhaxi Suo, 'Structural, Morphological and Magnetic Properties of Ni-Co Ferrites by the Mn^{2+} ions Substitution', Journal of Materials Science: Materials in Electronics, 30, 18729-18743 (2019).
15. Salar Ahmad, Sajjad Ali, Ikram Ullah, M.S Zobaer, Ashwag Albakri & Taseer Muhammed, 'Synthesis and Characterization of manganese Ferrite from Low Grade manganese ore through Solid State reaction route', Scientific Reports,11,16190 (2021).
16. Gaurav Yadav, Neeraj Kumar, Jyoti Shah, R.k. Konala & rekha Aggrawal ,'Enhancement in Magnetic and Dielectric Properties of Magnesium Ferrite by Lithium Substitution Applicable for High Frequency Shielding Material', Journal of Material Science and Mechanical Engineering, 3, 183-186 (2016).

17. G. Aravind, D. Ravinder & V. Nathanial, 'Structural and Electrical Properties of Li-Ni Nanoferrites synthesized by Citrate Gel Autocombustion Method', Physics Research International. Volume 2014, Article ID 672739,1-11.
18. W. R. Agami, M.A. Ashmawy, 'Structural, Physical and Magnetic Properties of Nanocrystalline Manganese-Substituted Lithium Ferrite Synthesized by Sol-gel Auto combustion Technique' Applied Physics A, 563, 1-9 (2020).
19. Sadaf Bashir Khan, Syed Irfan & Shern-Long Lee, 'Influence of Zn^{2+} Doping on Ni-Based Nanoferrites, ($Ni_{1-x}Zn_xFe_2O_4$)', Nanomaterials, 9, 1024 (2019).
20. Ali Bahadur, Aamer Saeed, Shahid Iqbal, Muhammed Saif Ur Rahman, Muhammad Imran Bashir, Muhammad Yaseen, Wajid Hussain, 'Morphological and Magnetic properties of $BaFe_{12}O_{19}$ Nanoferrite: A Promising Microwave Absorbing Material', Ceramics International, 43, 7346-7350 (2017).
21. G. Vasuki, T. Balu, 'Magnetic and Electrical Analysis of Chemically Derived $Cu_{0.5}Mn_{0.5}Al_{0.5}Fe_{1.5}O_4$ Nanocrystallites'. IJRAR, 5, 463-468 (2018).
22. Amer M.A, Meaz T.M, Attalah S.S, Ghoneim A.I, 'Structural Phase Transformation of as-prepared Mg-Mn Nanoferrites by Annealing Temperature', Materials Characterization, 110, 197-207 (2015).
23. P. Calandra, M. Goffradi, V. Turco Liveri, 'Study of the Growth of ZnS Nanoparticles in Water/AOT/n-heptane Microemulsions by UV-absorption Spectroscopy, Colloids and Surfaces' A: Physicochemical and Engineering Aspects, 160, 9-13 (1999).
24. Obaid Ur Rahman, Subash Chandra Mohapatra, Sharif Ahmad, 'Fe_3O_4 Inverse Spinel Super Paramagnetic Nanoparticles', Materials Chemistry and Physics,132, 196-202 (2012).
25. Mohamed A.Siddig, Abdalrawf I. Ahmed, Abdulmajid A. Mirghni, Abdelrahman A.Elbadawi, 'Structural and Optical Properties of $Mg_{1-x}Zn_xFe_2O_4$ Nanoferrites Synthesized Using Co-precipitaion method', Advances in Nanoparticles,4, 45-52 (2015).
26. Ephriam O Chukwuoccha, Michael Onyeaju, 'Theoretical Studies on the Effect of Confinement on Quantum Dots using the Brus Equation', World Journal of Condensed Matter Physics,2, 96-100 (2012).

27. G. Vasuki, T. Balu, 'Systematic Investigations on the Effect of Divalent Metal Ions (Mg^{2+} and Zn^{2+}) Substitution on Nanocrystalline Manganese Ferrites', Journal of Nano- and Electronic Physics, 11, 1-5 (2019).
28. Reetu Yadav, Radhika Batra, Priya Bansel and Roli Purwar, 'N-type Silk Fibroin/TiO_2 Nanocomposite Transparent Films: Electrical and Optical Properites', Polymer International 70, 1-12 (2021).
29. Gracia M, Marco J F, Gancedo J R, Ortiz J, Pastene R, Gautier J L, 'Characterization of the Lithium-Manganese Ferrite $LiFemnO_4$ Prepared by Two Different methods', The Journal of Physical Chemistry, 114, 12792-12799 (2010).
30. Paneer.I, Muthuselvam, BhowmiK R.N, 'Mechanical Alloyed Ho^{3+} doping in $CoFe_2O_4$ Spinel Ferrite and Understanding of Magnetic Nanodomains', Journal of Magnetism and Magnetic Materials,322, 767-776 (2010).
31. Mansour S.F, 'Structural and Magnetic Investigations of sub-nano Mn-Mg Ferrite Prepared by Wet Method', Journal of Magnesium and Magnetic Materials,323, 1735-1740 (2011).
32. K.M. Kosuda, J.M. Bingham, K.L.Wustholz, R.P. Van Duyne, R.J. Groarke, 'Nanostructures and Surface-enhanced Raman Spectroscopy', Comprehensive Nanoscience and Nanotechnology (Second edition), 4, 117-152 (2016).
33. Paramesh Donta, Vijaya Kumar Katrapally & Venkat Reddy Pendyala, 'Dielectric Response of $Ni_xZn_{1-x}AlFeO_4$ Nanoferrites', Nano World Journal, 2, 27-34 (2016).
34. Hajar Jalili, Bagher Aslibeiki, , Volodymyr, Chernenko A, 'The Effect of Magneto-Crystalline anisotropy on the properties of hard and soft magnetic ferrite nanoparticles', Beilstein Journal of Nanotechnology, 10, 1348-1359 (2019).
35. Gangatharan Sathishkumar, Chidambaram Venkataraju, Kundasamy Sivakumar, 'Synthesis, Structural and Dielectric Studies of Nickel Substituted Cobalt-Zinc Ferrite', Materials Sciences and Applications, 1, 19-24 (2010).
36. M. Kaiser, 'Structure, Electric and Dielectric Studies of Indium Substituted Magnesium Copper Manganese Ferrites', Physics B 406, 899-905 (2011).

37. S. Mahmood, S. Nasir, G. Asghar, M.Iftikhar, R. Hussain, G. Xing, ‘ Effect of Mg doping on Dielectric and Magnetic Properties of Co-Zn Nanoferrites, Journal of Ovonic Research, 15, 95-102 (2019).
38. Tsylya M. Levitskaya, Ben K. Sternberg, ‘Parameters describing the material behaviour in an electromagnetic field’, Electrical Spectroscopy of Earth Materials, 2019.
39. V. Vignesh, K. Subramani, M. Satish, R. Navamathavan, ‘ Electrochemical Investigations of Manganese Ferrites Prepared Via a Facile Synthesis Route for Supercapacitor Applications’, Colloids and Surfaces A, 538, 668-677 (2018).
40. Gita Singh, Sudeshna Chandra, ‘Electrochemical Performance of $MnFe_2O_4$ Nanoferrites Synthesized Using Thermal Decomposition Method’, International Journal of Hydrogen energy, 43, 4058-4066 (2018).
41. Wahran M.Saod, Layth L. Hamid, Nisreen Jassam Alaallah, Asmiet, Ramizy, ‘Biosynthesis and Antibacterial Activity of Manganese Oxide Nanoparticles Prepared by Green Tea Extract’, Biotechnology Reports, 34(2022).